JOURNAL OF Materials CHEMISTRY

# Coupling of the remanent polarisation in thin film oxide ferroelectrics with nematic liquid crystals

**John F. Hubbard,[a] Helen F. Gleeson,*[a] Roger W. Whatmore,[b] Christopher P. Shaw[b] and Qi Zhang[b]**

[a] *Department of Physics and Astronomy, Manchester University, Manchester, UK M13 9PL. E-mail: Helen.Gleeson@man.ac.uk*
[b] *Advanced Materials Group, SIMS, Cranfield University, Cranfield, Beds, UK MK43 0AL*

***Received 2nd October 1998, Accepted 10th November 1998***

The technique of domain visualisation, revealed by a film of nematic liquid crystal (NLC) on a ferroelectric crystal substrate, is demonstrated for the first time to be applicable to thin films of lead zirconate–lead titanate (PZT) ferroelectric ceramics. PZT film thicknesses $<1$ μm were deposited on indium tin oxide coated glass substrates. Commercially available NLC materials with positive dielectric anisotropy were employed. The electro-optic properties of devices incorporating the ferroelectric ceramic and NLC are reported. The poled PZT grains induce a local Fréedericksz transition in the NLC and it is proposed that the ferroelectric–NLC interaction is primarily due to the depolarisation field due to the ferroelectric remanent polarisation.

## Introduction

It has been known since 1973 that a thin film of nematic liquid crystal (NLC), when placed upon a ferroelectric crystal, is able to delineate the domain structure of the underlying crystal substrate.[1–10] This phenomenon was first demonstrated by Furuhata and Toriyama for the ferroelectric crystal triglycine sulfate (TGS) and the NLC *p*-*N*-(*p*-methoxybenzylidene)amino-*n*-butylbenzene.[1] They proposed a model whereby the spontaneous polarisation of a ferroelectric domain couples with the dipole moment of the NLC allowing parallel and anti-parallel domains to be distinguished using polarising microscopy. This so-called *domain visualisation technique* has since been used to observe the static domain structure of other ferroelectric crystals such as $NaNO_2$,[5,6] $Li_2Ge_7O_{15}$[8] and $LiH_3(SeO_2)_3$[11] as well as the dynamic switching of ferroelectric domains for TGS,[3] $NaNO_2$[5,6] and $(CH_3NH_3)_5Bi_2Br_{11}$.[7] More recently the coupling mechanism between the domains of ferroelectric crystals with NLC has been described in terms of the dielectric anisotropy of the NLC, $\Delta\varepsilon$, the cohesive energy of the crystal surface and the symmetry of the ferroelectric crystal.[4]

To date, the domain visualisation technique has only been applied to ferroelectric crystalline materials of thickness 0.05–10 mm. The results presented in this paper demonstrate that this technique may be extended to include oxide ferroelectric (OFE) films of submicron thickness. NLC materials of positive dielectric anisotropy are shown to interact with the poled grains of a thin film of lead zirconate–lead titanate, $Pb(Zr_{0.30}Ti_{0.70})O_3$ (PZT 30/70). The visualisation technique is shown to provide a valuable way of observing the poled domain structure in OFE thin films.

## Theory

In order to investigate the interactions between the poled regions of a thin film OFE ceramic and a NLC layer, the schematic device geometry shown in Fig. 1 was considered. The inner surfaces of the upper indium tin oxide (ITO) coated glass and lower OFE/ITO glass substrates were coated with thin ($<0.1$ μm) layers of rubbed poly(vinyl alcohol) (PVA) to provide a uniform, parallel orientation of the NLC director with the surfaces. Treating the surfaces in this way ensures that the interaction of the NLC with the OFE must be through

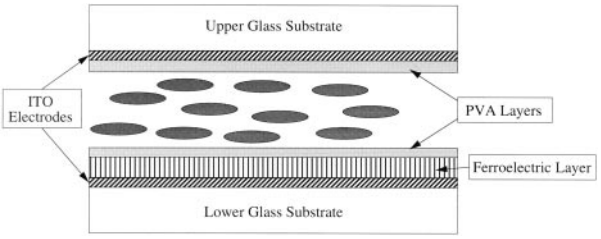


**Fig. 1** Schematic representation of the OFE/NLC device investigated. The diagram is not to scale and the dimensions of the layers are typically as follows: glass substrate, 1 mm; OFE layer, 0.5 μm; NLC layer, 5 μm; PVA layer, $<0.1$ μm. The rubbing direction and hence the NLC director $\tilde{n}$ are from left to right.

the OFE remanent polarisation since the PVA layer provides the direct surface interactions. Further, the well defined device geometry allows the interaction of the NLC layer with the OFE to be quantified, as will be discussed. (The term 'remanent polarisation' will be used in this paper, rather than 'spontaneous polarisation', because it refers to the polarisation remaining in the ferroelectric after the poling voltage has been removed. The term 'spontaneous polarisation' really refers to the intrinsic lattice polarisation of the ferroelectric, which is only achieved in a fully polarised material, which we never achieve in these experiments.)

The device comprises four dielectric layers; the OFE, the lower PVA layer, the NLC layer and the upper PVA layer. The electrical properties of the PVA are comparable with those of the NLC, the dielectric permittivity and resistivity being approximately 10 and $10^{10}\,\Omega\,m$ respectively in both cases. Because of the electrical similarity of these layers, it is possible to consider the contribution of the PVA layers ($<0.1$ μm thick) to the characteristics of the device as a whole as an insignificantly small increase in the layer thickness of the NLC (typically between 5 and 10 μm thick). Hence, as a first approximation the electrical characteristics of the device may be modelled by considering only two dielectric layers in a series circuit as shown in Fig. 2.

The NLC and OFE layers have associated with them a resistive element, $R_{LC}$ and $R_{OFE}$, as well as a capacitive element $C_{LC}$ and $C_{OFE}$, where the subscripts refer to the NLC and OFE layers respectively. If a sinusoidal voltage is applied to the device shown in Fig. 1 then the impedance of each layer,

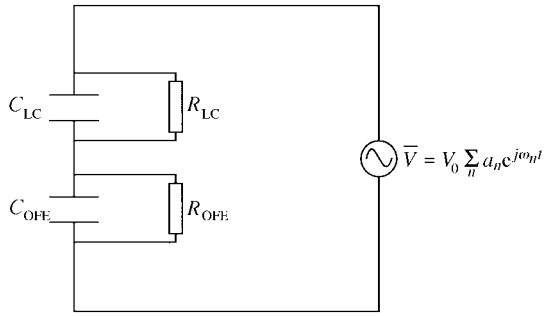


**Fig. 2** The equivalent circuit of the OFE/NLC device shown in Fig. 1, where $\bar{V}$ is the applied sinusoidal voltage. The capacitances and resistances of the layers are indicated by $C$ and $R$, respectively, with the appropriate subscript.

$\bar{Z}_i$, may be written as

$$\bar{Z}_i = -jR_i/\omega C_i(R_i - j/\omega C_i) \quad (1)$$

where $i$ is LC or OFE, depending on the layer type. The voltage across the OFE layer, $\bar{V}_{OFE}$, can be expressed as

$$\bar{V}_{OFE} = \bar{V}/[(\bar{Z}_{LC}/\bar{Z}_{OFE}) + 1] \quad (2)$$

as it can be shown that

$$\frac{\bar{Z}_{LC}}{\bar{Z}_{OFE}} = \frac{\rho_{LC} t_{LC}}{\rho_{OFE} t_{OFE}} \frac{(\omega^2\tau^2_{OFE} + 1)}{(\omega^2\tau^2_{LC} + 1)} \frac{[1 - j\omega\tau_{LC}]}{[1 - j\omega\tau_{OFE}]} \quad (3)$$

where $\rho_{LC}$, $t_{LC}$ and $\tau_{LC}$ are the DC resistivity, thickness and material time constant of the NLC (defined as a $\rho_{LC}\varepsilon_{LC}\varepsilon_0$ where $\varepsilon_{LC}$ and $\varepsilon_0$ are the relative permittivity of the NLC and free space, respectively). Similar parameters are defined for the OFE layer in eqn. (3) by the quantities with the subscript OFE.

The anisotropic NLC layer has two dielectric constants associated with it, one parallel and one perpendicular to the director ($\varepsilon_\parallel$ and $\varepsilon_\perp$ respectively); $\varepsilon_\parallel$ is the appropriate one to include in eqn. (3) since the voltages that are applied to create the fields necessary to pole the OFE are well above the switching threshold of the NCLs which is usually of the order of 1 $V_{rms}$ at 1 kHz). Further, the poling voltage is applied for several seconds, much longer than the reorientation time of the NCL (typically around 1 ms).

Consider the case where a relatively high frequency voltage of 1 kHz is applied to the device. Then, the voltage appearing across the OFE layer is

$$|V_{OFE}| = V_0 \Big/ \left[1 + \frac{\varepsilon_{OFE} t_{LC}}{\varepsilon_{LC} t_{OFE}}\right] \quad (4)$$

where $V_0$ is the driving voltage. The OFE used in this work was the lead zirconate–lead titanate [$Pb(Zr_{1-x}Ti_x)O_3$] system with the composition $Pb(Zr_{0.30}Ti_{0.70})O_3$, denoted PZT (30/70). The NLCs used were commerically available[12] with a positive dielectric anisotropy ($\Delta\varepsilon = \varepsilon_\parallel - \varepsilon_\perp > 0$). The OFE and NLC materials are listed in Table 1 together with their respective dielectric constants ($\varepsilon$), resistivities ($\rho$), time constants ($\tau$), remanent polarisations ($P_r$) and coercive fields ($E_c$).

In order to induce a bulk remanent polarisation of the PZT (30/70), and hence observe its influence on the overlying NLC, the voltage across the OFE layer in the device must be of the order of the coercive field, *i.e.* 5 V $\mu m^{-1}$. From eqn. (4) it is apparent that $|V_{OFE}|$ is dependent on the dielectric constants and thickness of both layers as well as the driving voltage. Using the above equations, the voltages applied to the ferroelectric layer can be calculated for specific device structures and poling regimes.

**Table 1** Electrical properties of the NLCs and OFE investigated; note that $\varepsilon$ for the NLCs is that for $\varepsilon_\parallel$ measured[12] at 20 °C (at 1 kHz)

| | E7 | MLC 6204 000 | PZT (30/70) |
|---|---|---|---|
| $\varepsilon$ | 19.0 | 44.8 | 230 |
| $\rho/\Omega$ m | $\sim 10^{10}$ | $\sim 10^{10}$ | $10^9$ |
| $\tau$/s | $\sim 1.7$ | $\sim 4.0$ | 2 |
| $P_r$/C $m^{-2}$ | — | — | 200 |
| $E_c$/V $\mu m^{-1}$ | — | — | 0.50 |

## Experimental

PZT (30/70) was deposited onto ITO coated glass by a sol–gel/spin-coating procedure[13] resulting in a film thickness in the range 0.15–0.50 μm as confirmed by a combination of scanning electron microscopy and Talysurf™ (Rank Taylor Johnson) measurements. The perovskite nature of the PZT films was confirmed with a Phillips PW1720 X-ray diffractometer, operating at 1.789 Å (iron filtered cobalt Kα, slit width 0.05 mm). Fig. 3 shows a typical X-ray diffraction plot of a PZT (30/70) film of thickness 0.26 μm (see Table 2 for the assignments of peaks). The dielectric properties, resistivity and hysteretic properties of the films were determined using a GenRad 1689M RLC Digibridge, Keithley Model 6517 Electrometer and Radiant Technologies RT66A loop tracer respectively. The values determined are those cited in Table 1.

The ITO and PZT were removed from the edges of the upper and lower substrates producing active electrode areas of 10–25 $mm^2$. The removal of the ITO avoided electrical breakdown of air (the breakdown field is between 1 and 3 V $\mu m^{-1}$) at the device edge during the application of electric fields to the device. Antiparallel NLC director alignment was achieved with unidirectionally rubbed PVA. Polyethyleneterephthalate spacers were used to maintain well defined spacing between the substrates in the range 4–15 μm. The device edges were sealed with Araldite® epoxy leaving a small hole along one edge to enable filling. The thickness of the device was measured before filling to an accuracy of $\pm 0.25$ μm using spectrophotometry. The devices were filled with NLC in vacuum to minimise the presence of air. Wires were attached to the electrodes on the substrates using indium solder.

The devices were observed using an Olympus BH-2 polarising microscope with the device alignment direction at 45° to the crossed polarisers. Sinusoidal voltages of up to 650 $V_{rms}$, with frequency in the range 1–5 kHz, were applied to the devices using an in-house built high voltage amplifier connected to a programmable function generator. The voltages necessary to pole the OFE layer were applied for 1–3 s. After the poling fields were removed, the devices were left for typically 5 s before photographs of the electrode area of the device were taken. The long time delay between poling the device and subsequent observations ensured that no transient effects due to ionic conduction or defect motion in the device could account for the observations made.

## Results

Numerous hybrid NLC devices were fabricated as described in the previous section where the PZT thickness varied from 0.15 to 0.50 μm and that of the NLC varied from 4 to 15 μm. Direct observation of the devices prior to poling confirmed that the alignment of the NLC layer was uniform.

An important characteristic of the PZT films which has not been discussed so far relates to the size of the grains. Fig. 4 shows an optical photomicrograph of a PZT film of thickness 0.34 μm (parallel polarisers) where the grain size is of the order of 5 μm. The contrast at the grain boundaries is thought to originate from the presence of pyrochlore phase in that region. The grain size was found to depend on firing time and firing temperature of the films, the grains reaching their maximum size after typically 12–13 min at 512 °C.

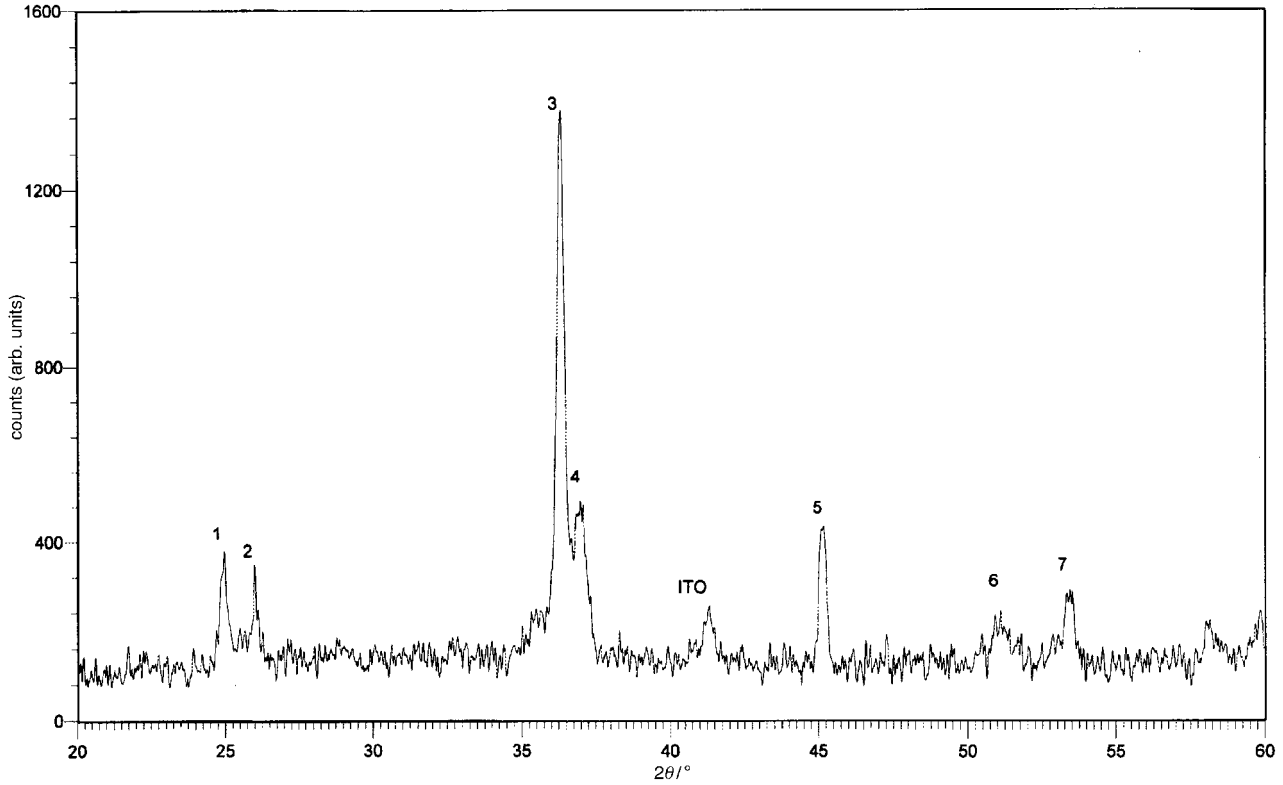


**Fig. 3** X-Ray diffraction plot for a PZT (30/70) film of thickness 0.26 μm.

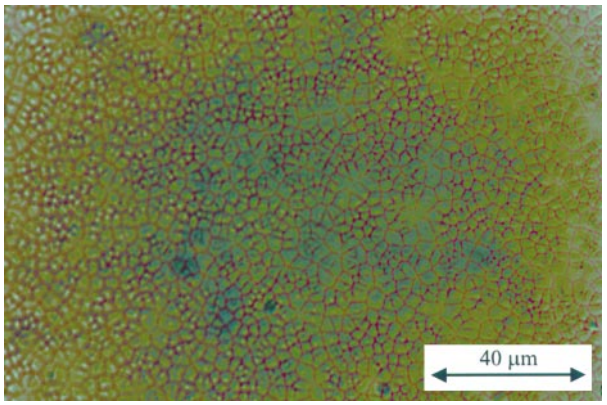


**Fig. 4** Photomicrograph of a PZT film of thickness 0.34 μm, parallel polarisers, 30 °C.

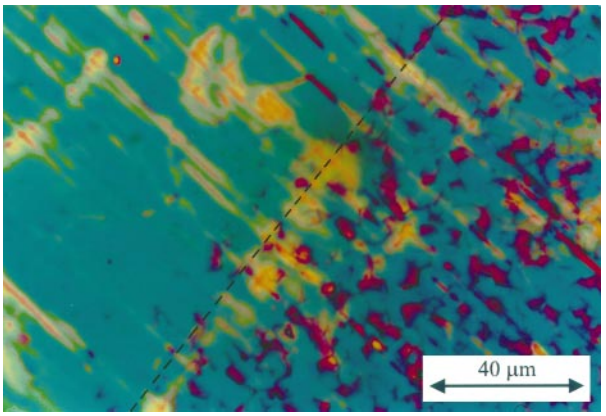


**Fig. 5** Photomicrograph of the electrode edge of a device comprising 4.2 μm of MLC 6204000 and 0.26 μm PZT after a poling voltage of 150 $V_{rms}$ (at 1 kHz) has been applied. Crossed polarisers, 30 °C.

Prior to poling the PZT film there is no bulk remanent polarisation. This is because within each grain there is a fine (sub-micron scale) structure of 90 and 180° domains. This structure is not visible optically, although it has been observed by transmission electron microscopy (TEM).[14]

As already mentioned, although the PVA layer provides the direct surface coupling with the NLC, any field appearing at the surface of the ferroelectric due to a net remanent polarisation within the PZT grains will have a component that leaks through the PVA layer. If this field is sufficiently large it will interact with the NLC by causing a Fréedericksz transition and the polarised grains will thus be visualised. This effect is discussed further below.

Evidence that after application of a poling field the PZT interacts with the overlying NLC is provided by Fig. 5 in which the edge of the electrode area has been indicated by a dashed line. The plate shows the appearance of a device comprising 4.2 μm of MLC 6204000 and 0.26 μm of PZT several seconds after a poling voltage pulse of duration approximately 3 s and amplitude 150 $V_{rms}$ (at 1 kHz) was applied to the device. In many of the PZT grains, the birefringence colour of the NLC has been altered from a blue to a red colour. The region within the electrode area shows numerous 'red coloured' PZT grains whereas outside this area there are very few red grains. This indicates that coupling of the PZT grains with the NLC has been caused by the effect of the applied electric field, presumably as a result of an induced remanent polarisation within those grains. The magnitude of the voltage pulse applied in relation to the coercive field of the PZT grains is discussed further below.

The optical properties of the device are dominated by the NLC layer since the optical retardance is much greater for the NLC layer ($\Delta n = 0.1478$ for MLC 6204000 and $t_{LC} \approx 5$ μm) than for the PZT. The contribution to the retardance of the PZT is negligible since the maximum birefringence (for a grain with the *c*-axis parallel to the substrate and at 45° to the crossed polarisers) is 0.01, the film thickness is $<0.5$ μm, so the retardance of the PZT film is $<0.5\%$ of that of the NLC film. Above the poled PZT grains, the birefringence colour

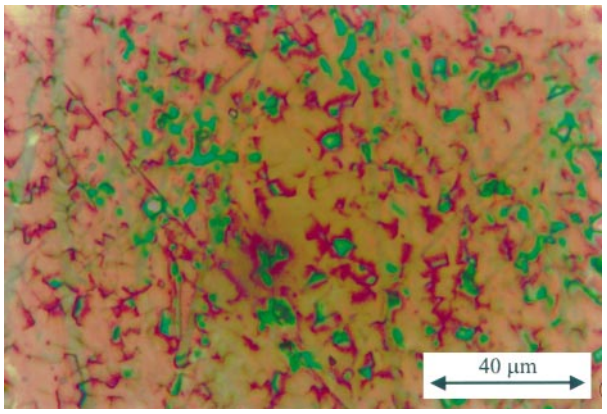


**Fig. 6** Photomicrograph of the electrode edge of a device comprising 8.85 μm of E7 and 0.26 μm PZT after a poling voltage of 640 $V_{rms}$ (at 1 kHz) has been applied. Crossed polarisers, 30 °C.

has changed from blue to red, as can be seen in Fig. 5. Rotation of the microscope hot stage confirmed that there was no reorientation of the NLC optic axis in the plane of the device so the change in colour can be attributed entirely to reorientation of the NLC in a plane perpendicular to the substrates. This is also discussed in more detail below.

The PZT grain–NLC interaction has also been observed for the mixture E7 as shown in Fig. 6. Here, the device comprised 8.9 μm of E7 and 0.26 μm of PZT. The poling voltage applied was 640 $V_{rms}$ at 1 kHz.

## Discussion

In order to understand the poled PZT-NLC interaction one must first consider the structure of the ferroelectric ceramic film. Fig. 7(a) shows a schematic representation of the hybrid device before a poling field has been applied. [Here, the unpoled crystals are shown schematically as blocks with sets of anti-parallel arrows. Their actual structure is as shown schematically in Fig. 7(c).] The deposition of PZT onto ITO coated glass is known from the X-ray diffraction studies to produce plate-like crystallites with a random orientational distribution of the tetragonal perovskite *c*-axis (polarisation axis), see Fig. 3 and Table 2. This can be interpreted such that within each grain there exists a fine lamellar structure of 90 and 180° ferroelectric domains (having a net zero bulk remanent polarisation within each grain before poling). However, the orientation of the polar axes varies from grain to grain across the whole film. Since there is no bulk remanent polarisation of any grain, and hence the whole film, there is no coupling of the PZT grain structure to the NLC director, $\tilde{n}$.

If we consider the case of the device using the MLC 6204 000 liquid crystal shown in Fig. 5, then it is easy to show from eqn. (4), the device dimensions listed above and the materials properties listed in Table 1 that the field drop across the ferroelectric layer is 9.7 $V_{pp}$ $\mu m^{-1}$, or about one half of the coercive field. It is worth noting at this point that the term 'coercive field' ($E_c$) when applied to a ferroelectric is *not* the field required to 'switch' the ferroelectric, but is the field required to reduce the net remanent polarisation of a fully poled ferroelectric to zero. (Typically, the field required to fully pole a polycrystalline ferroelectric will be two or three times $E_c$.) However, because of their orientations and stress environments, some grains will be far more easily poled than others and a significant number will be poled by fields which are much smaller than $E_c$. It is believed that this is what we are observing in this specimen. Inspection of Fig. 5 shows that about 20–25% of the grains are switched, which is in line with the net field applied to the ferroelectric layer. If we consider the device made with E7 liquid crystal, the field across the

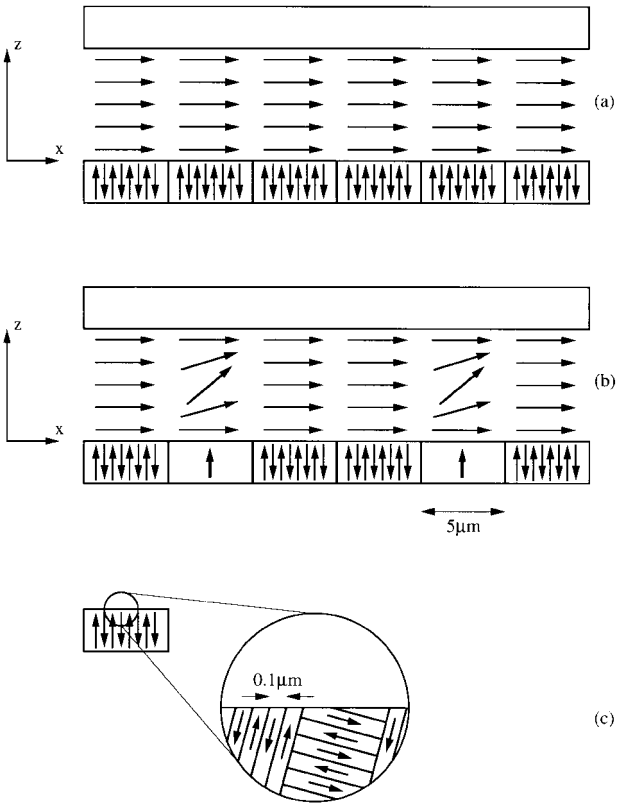


**Fig. 7** A model representing the coupling mechanism of poled grains of PZT with NLCs. The small arrows represent the ferroelectric domains with the grains of the PZT, whereas the larger arrows indicate the nematic director orienation. (a) The device prior to poling, (b) the device after a poling field has been applied and some of the grains are poled, (c) the substructure of the ferroelectric grains.

**Table 2** X-Ray diffraction data obtained for a PZT (30/70) film of thickness 0.26 μm (plot shown in Fig. 3)

| Peak number | Angle, $2\theta$/° | Counts/ arb. units | *D*-space/ Å | Relative intensity/ arb. units | Miller index |
|---|---|---|---|---|---|
| 1 | 24.96 | 381 | 4.139 | 28 | 001 |
| 2 | 25.98 | 349 | 3.979 | 25 | 100 |
| 3 | 36.29 | 1377 | 2.872 | 100 | 101 |
| 4 | 37.06 | 485 | 2.815 | 35 | 110 |
| 5 | 45.07 | 418 | 2.334 | 29 | 111 |
| 6 | 50.91 | 237 | 2.081 | 17 | 002 |
| 7 | 53.33 | 284 | 1.993 | 21 | 200 |

ferroelectric layer is 8.3 $V_{pp}$ $\mu m^{-1}$, slightly less than the other device and here it does appear that significantly fewer grains are poled by the process. It is interesting to consider the charge flows and fields associated with a single polarised grain. Assuming the properties given in Table 1, it is simple to show that the depolarisation field ($E_d$) within the ferroelectric as a consequence of the remanent polarisation is *ca.* 200 MV $m^{-1}$ (this occurs in all ferroelectrics and is given by $E_d = -P_r/\varepsilon\varepsilon_0$[15]). After poling, free charges will flow within the ferroelectric to tend to neutralise the remanent polarisation and hence the surface potential. The time, $t_\zeta$ taken to reduce the polarisation to a fraction $\zeta$ of $P_r$ due to charge flow within the ferroelectric will be given by $t_\zeta = \varepsilon\varepsilon_o\rho\ln(\zeta^{-1}) = \tau_{OFE}\ln(\zeta^{-1})$. Typically, this time will be about 43 s to reduce the surface potential to 0.1 V. This point is discussed further below.

The NLC above those grains which have been poled will experience a small electric field. Coupling between this field and the positive dielectric anisotropy of the NLC results in a change in the birefringence colour observed and corresponds to a tilt of $\tilde{n}$ in the plane perpendicular to the device substrate.

Such field induced deformations of NLCs are usually termed Fréedericksz transitions.[16] Here, it is appropriate to call this grain induced birefringence change above poled PZT grains a *local* Fréedericksz transition. It is apparent that since not all crystallites within the PZT film have their crystallographic directions favourably oriented for switching with respect to the applied field direction, and only a fraction of the coercive field has been applied, one would only expect to pole a fraction of the grains and it is observed that the birefringence of the NLC changes only above some grains. Poling with ac fields will result in some grains possessing a remanent polarisation in either the $+z$ or $-z$ directions [Fig. 7(b)], which would affect the non-polar NLC materials identically, amid a majority of unpoled grains. The structure of the unpoled grains and the way in which this will affect the NLC deserves some discussion. As noted above, these grains consist of a fine (submicron scale) lamellar structure of 90 and 180° domains, as shown schematically in Fig. 7(c). The domain structure will organise itself to minimise the depolarisation and mechanical strain energies[14] and the penetration of the electrostatic field from the surface of the domains into the NLC can be no greater in depth than the size of the domains at the surface. It is most likely that the effect of the extremely fine domain structure in these crystallites is effectively to present a uniform, zero polarisation surface to the NLC, giving the uniform colour observed between the poled grains in Fig. 5 and 6.

The model presented in Fig. 7 is, we believe, the most likely mechanism for coupling the spontaneous polarisation of the poled PZT grains with the NLC. Because of the well defined device geometry, it is possible to model the director tilt and thus gain a more detailed insight into the OFE/NLC interaction. The magnitude of detector tilt can be determined by applying a small driving voltage ($\approx 1$ $V_{rms}$) to the device which causes the entire NLC area to undergo a Fréedericksz transition. Measuring the voltage at which the original birefringence colours of the poled grains matches that of the surrounding area allows the director tilt to be deduced.[16,17] Such measurements on various devices constructed using the OFE and NLC materials indicate that the binding energy contribution is significant and infinite anchoring cannot be assumed. Although further work is required in order to confirm the correct coupling mechanism, it is possible to gain some significant insight into them through estimates of the surface anchoring energies. Since there is no twist distortion of the nematic director, the surface anchoring energy $W^{\theta}$ may be calculated from[16] $W^{\theta}=\pi^2 t(k_{11}+k_{33})/2{d_B}^2$, where $k_{11}$ and $k_{33}$ are the splay and bend elastic constants of the NLC, $t$ is the thickness of the LC layer and $d_B$ is the thickness of the domain wall that occurs between the area of the NLC that experiences a local Fréedericksz transition and the surrounding unchanged area. Observation of the various devices studied leads to $d_B$ of between 2 and 5 μm, resulting in anchoring energies of between 5 and $10\times10^{-2}$ erg cm$^{-2}$. This compares with $2.1\times10^{-2}$ erg cm$^{-2}$ reported for the nematic liquid crystal MBBA on the ferroelectric crystal triglycine sulfate.[18] A number of factors will affect anchoring energy. However, if the depolarisation field is playing a major role in the orientation of the liquid crystal, as suggested here, it would be expected to affect the binding energy. The magnitude of any surface field which will interact with the NLC should thus be proportional to the ratio of the remanent polarisation to the dielectric constant in the ferroelectric substrate (see equation given for $E_d$ above). The properties of the OFE system studied here are compared with that reported by Gunyakov *et al.*[18] in Table 3. It can be seen that the ratios of $P_r/\varepsilon$ for TGS and PZT compare well with the ratios of the binding energies. While the binding energy data are preliminary, it is felt that this is reasonably good evidence that the OFE/NLC interaction is dominated by the depolarisation field in the OFE. Other authors have not discussed in detail the nature of this interaction. However, it is likely to be electrostatic in nature. This is borne out by our experiments in which there is a PVA layer between the ferroelectric and the NLC, so there cannot be any direct chemical interaction between them.

**Table 3** A comparison of the binding energy of NLCs with different ferroelectric substrates

| Material | $P_r$/μC cm$^{-2}$ | Permittivity/$\varepsilon$ | $P/\varepsilon$ | $E_b/10^{-2}$ erg cm$^{-2}$ |
|---|---|---|---|---|
| TGS[18] | 2.8 | 43 | 0.065 | 2.1 |
| PZT 30/70 | 50 | 230 | 0.22 | 5–9 |

One factor still open to question is why the effect does not disappear with time as the movement of charges within the ferroelectric tends to neutralise the depolarisation field, which we would expect to happen on a time scale of minutes. The grains showing altered birefringence colours were stable for months. In fact, there were no devices which had been 'poled' in which the remanent polarisation interacted with nematic where the poled regions reverted back to their original colour. It may be that the free charges moving within the ferroelectric effectively get trapped at defects (dislocations, grain boundaries *etc.*) within the bulk of the material, neutralising the bulk depolarisation field, but still leaving a free electrostatic dipole at the surface of the ferroelectric to interact with the NLC. However, this is largely speculation at this stage and the issue must await the results of further work to be resolved.

Apart from being intrinsically interesting, these observations could have some technological importance. The study of ferroelectric thin films is important for integrated memory and sensor applications and the NLC method could be useful in helping to understand the switching phenomena in these materials. Furthermore, there are studies in progress on the use of ferroelectric films on alumina substrates in xerographic printing applications.[19] Here, toner particles are selectively attracted to poled regions of a ferroelectric layer and here, again, the phenomenon shows long term stability and although stable surface-potential measurements after poling of hundreds of volts have been made, little is understood about the basic physics of the phenomenon. These NLC–OFE film interaction studies could help to shed light upon the effect.

## Summary and conclusions

It has been demonstrated that the well known technique of domain visualisation as applied to ferroelectric crystals and NLCs may be extended to include thin film oxide ferroelectric ceramics as the substrate. Hybrid devices comprising thin film PZT and various NLCs have been constructed. By considering such devices as two dielectrics in series, a model was described whereby the PZT layer can be poled by applying a high frequency sinusoidal electric field across the layers. The poled grains of the PZT were observed to induce contrast in the NLC which is explained by the occurrence of 'local Fréedericksz transitions' in the NLC layer above those grains which possess ferroelectric domains collinear with the applied field direction. These 'local Fréedericksz transitions' are more noticeable for large grained PZT (*i.e.* $>5$ μm). The grain structure makes quantifying the OFE–NLC interaction difficult, and work with other substrates such as magnesium oxide (MgO), on which it is known that PZT can be deposited with an epitaxial *c*-axis orientation[19] is underway. A preliminary comparison of the anchoring energies of the OFE–LC systems studied here with those published elsewhere for organic ferroelectric crystals implies that the anchoring energy of the NLC is dominated by the depolarisation field of the ferroelectric. These results provide the first evidence that it is possible to couple the poled regions of thin film PZT with a NLC. A full study of the interactions of NLCs with poled OFEs is underway and will be the subject of future publications.

## Acknowledgements

The authors would like to thank the EPSRC (grants GR/K/89665 and GR/M03993) for the funding of this work. R. W. W. would like to thank the Royal Academy of Engineering for their financial support.

## References

1 Y. Furuhata and K. Toriyama, *Appl. Phys. Lett*., 1973, **23**, 361.
2 V. P Konstantinova, N. A. Tikhomirova and M. Glogarova, *Ferroelectrics*, 1978, **20**, 259.
3 N. A. Tikhomirova, L. A. Shuvalov, A. I Baranov, A. R. Karesev, L. I. Dontsova, E. S. Popov, A. V. Shilnikov and L. G. Bulatova, *Ferroelectrics*, 1980, **29**, 51.
4 L. I. Dontzova, N. A. Tikhomirova and L. A. Shuvalov, *Ferroelectrics*, 1989, **97**, 87.
5 V. V. Galtsev, N. A. Nedostup, N. R. Ivanov and N. A. Tikhomirova, *Ferroelectrics*, 1990, **111**, 217.
6 J. Hatano, R. Le Bihan, F. Aikawa and F. Mbama, *Ferroelectrics*, 1990, **106**, 33.
7 M. Polomska and R. Jakubas, *Ferroelectrics*, 1990, **106**, 57.
8 N. A. Tikhomirova, A. V. Ginzberg, S. P. Chumakova, M. D. Volnyanskii, M. Polomska and P. V. Adomenas, *Ferroelectrics Lett.*, 1991, **13**, 81.
9 V. A. Gunyakov, A. M. Parshin, B. P. Khrustalev and V. F. Shabanov, *Solid State Commun*., 1993, **87**, 751.
10 V. A. Gunyakov, A. M. Parshin, B. P. Khrustalev and V. F. Shabanov, *J. Opt. Technol.*, 1997, **64**, 483.
11 V. N. Anisimova, N. A. Tikhomirova and L. A. Shuvalov, *Tesisi XI Vsesoyuznogo soweszanija po segnetoeletrichestvu*, Rostov-na-Donu, Sept. 1979, vol. 1, p. 144.
12 Business Unit Liquid Crystals, Merck, Darmstadt, Germany.
13 D. A. Tossel, J. S. Obhi, N. M. Shorrocks, A. Patel and R. W. Whatmore, *Proc. 8th Int. Symp. Appl. Ferroelectrics*, Greenvill, SC (IEEE Cat. No. 9ZCH3080–9), p. 11; A. Patel, E. A. Logan, R. Nicklin, N. B. Hasdell, R. W. Whatmore and M. Uren, *Mater. Res. Soc. Symp. Proc*., 1993, **310**, 447.
14 S. A. Impey, Z. Huang, A. Patel, R. Beanland, N. M. Shorrocks, R. Watton and R. W. Whatmore, *J. Appl. Phys.*, 1998, **83**, 2202.
15 M. E. Lines and A. M. Glass, *Principles and Applications of Ferroelectrics and Related Materials*, OUP, Oxford, 1977.
16 See for example L. M. Blinov and V. G. Chigrinov, *Electrooptic Effects in Liquid Crystal Materials*, Springer, Berlin, 1996.
17 G. Vertogen and W. H. de Jeu, *Thermotropic Liquid Crystals, Fundamentals*, Springer Verlag, Berlin, 1988.
18 V. A. Gunyakov, A. M. Parshin and V. F. Shabanov, *Solid State Commun.*, 1998, **105**, 761.
19 A. Hirt, *Integr. Ferroelectrics*, 1995, **10**, 319.

*Paper 8/07684G*